GeoScienceWorld
Lithosphere
Volume 2023, Article ID lithosphere_2023_110, 15 pages
https://doi.org/10.2113/2023/lithosphere_2023_110

Lithosphere

Research Article

Lithospheric Structure and Extensional Style of the Red Sea Rift Segments

Kuruvamana Satheeshbabu Sreenidhi,[1,2,3] **Munukutla Radhakrishna**,[2] **and Peter G. Betts**[3]

[1]*IITB-Monash Research Academy, Indian Institute of Technology Bombay, Mumbai, Maharashtra, India*
[2]*Department of Earth Sciences, Indian Institute of Technology Bombay, Mumbai, Maharashtra, India*
[3]*School of Earth, Atmosphere, and Environment, Monash University, Clayton, Victoria, Australia*

Correspondence should be addressed to Kuruvamana Satheeshbabu Sreenidhi; sreenidhi.iitbmonash@gmail.com

Received 2 February 2023; Accepted 4 October 2023; Published 30 October 2023

Academic Editor: Songjian Ao

The Red Sea provides an opportunity to study the processes during the transition from continental rifting to early-stage seafloor spreading during ocean initiation. We delineate variations of lithospheric architecture and the nature of extension along the Red Sea region through joint interpretation of gravity and geoid anomalies and gravity-topography transfer functions. We use lithospheric-scale models to compare stretching factors with upper mantle gravity anomaly, residual mantle Bouguer anomaly, and effective elastic thickness. Based on our observations, the Red Sea is divided into four segments; each having distinct lithospheric characteristics and stretching styles. These are: (i) southernmost Red Sea and Danakil having regionally weak and stretched lithosphere, (ii) southern Red Sea with fully developed seafloor spreading and asymmetric lithospheric architecture, (iii) central Red Sea having discontinuous magma accretion with newly formed seafloor spreading, and (iv) northern Red sea with a stronger lithosphere and limited stretching revealing a stage of continental rifting. In these segments, lithospheric stretching correlates with regions of weak lithosphere, including a regime of sublithospheric plume channel beneath the southern Red Sea. The Zabargad fracture zone between the central and northern segments is revealed as a major lithosphere-scale boundary that may act as a barrier to the propagation of seafloor spreading into the northern Red Sea. The weak and highly stretched lithosphere in this region may indicate the onset of a new spreading cell. Our results conclude that the evolution of the Red Sea is more complex than the previously suggested kinematic models of simple "unzipping" and illustrate that several extensional styles can exist within different segments during the initial stages of ocean formation.

1. Introduction

The Red Sea represents a divergent tectonic boundary that is transitioning from a continental rift to an incipient oceanic basin. Given its distinctive stage of development as an oceanic basin, the Red Sea serves as a natural laboratory for investigating the intricate processes associated with continental rifting and ocean initiation. Despite extensive geological [1–4] and geophysical [5–10] studies, the geodynamics and crustal architecture of the Red Sea remain debated. Different propositions concerning the style and mode of extension and subsequent basin formation in the Red Sea include multistage pull-apart [11], asymmetric [12–14], and symmetric [15] rifting. Similarly, there is no consensus, from previous studies, on the extent of seafloor spreading [5–9, 16–21], the influence of the Afar plume or far-field forces in the Red Sea opening [22], and the role of lithospheric heterogeneities in the basin evolution [23–25].

We delineate the lithospheric architecture along the Red Sea through constrained topography-gravity-geoid modeling and analyze the variations in crustal and lithospheric stretching factors to understand the segmentation and modes of extension along the Red Sea. The results are compared with maps of an estimated effective elastic

thickness (Te), upper mantle gravity (UMG), and residual mantle Bouguer anomalies (RMBA) to infer controls on rifting in different segments of the Red Sea. Our results provide insights into the ocean initiation process and a link between Red Sea evolution, rheology and upper mantle structure.

2. Datasets

We utilized regional and global topography, gravity, geoid, seismic, seismological, and well data from the Red Sea and the adjoining continents (Figure 1(a)–1(c)). Regional topography data were extracted from the ETOPO1 global relief grid with a 1′×1′ spatial resolution [26]. Gravity anomalies were derived from the satellite global free-air gravity grid from the V23.1 gravity database [27], and the geoid data were taken from the Earth Geo-potential Model EGM2008 grid [28]. These global grids have a 1′×1′ spatial resolution and contain wavelength information sufficient for regional geophysical investigations [29]. We compiled available seismic reflection and refraction data, results from receiver function studies, and well data for constraining lithospheric geometry during 2D modeling (Figure 1(c) and Table S1 in supporting information S1). The global upper mantle shear-wave velocity model SL2013sv [30] was used to compute UMG effects.

3. Methods of Analysis

Three independent approaches were adopted to analyze geophysical datasets to understand the lithospheric structure and the rheological characteristics of the Red Sea.

3.1. Joint Topography-Gravity-Geoid Modeling. The joint topography-gravity-geoid models provide different scales of subsurface information. This approach, if properly constrained, generates robust lithospheric models as the geoid is sensitive to deeper mass anomalies, whereas crustal-scale mass heterogeneities are reflected in the gravity data [31]. To delineate the lithospheric architecture and its variation both along and across the Red Sea region, we extracted twenty profiles across the Red Sea (Figure 1(b)) for the seismically constrained modeling. Each profile extends from the African to Arabian continental interior perpendicular to the Red Sea margin. The profiles are ~700 km long and spaced 90–100 km apart.

We computed Bouguer gravity anomalies from the free-air gravity grid by assuming average density values for water, continental, and oceanic crust (Table S2 in supporting information S1). The residual geoid grid was prepared by subtracting the long-wavelength contribution up to degree 10 (referred to as degree-10 residual geoid) from the full-spectrum grid to obtain information on lithospheric mass variations. The forward modeling involved matching the model responses with observed topography, degree-10 residual geoid, and the Bouguer gravity data. We modeled the layers of water, sediments, oceanic crust, upper and lower continental crust, and lithospheric and asthenospheric mantle. Underplated crust and intrusions were included in several models to determine a suitable model fit. The modeled underplate layers were incorporated into the lower crust assuming that the associated igneous component of the model formed during the rifting and requires a similar mode of isostatic compensation as for the stretched region [32]. Values of lithological properties used in the modeling are given in Table S2 in supporting information S1.

Seismic, seismological, and well data were used to constrain the crustal structure and the Lithosphere-Asthenosphere Boundary (LAB) depth. The seismic constraints within a distance of 50 km from each of the profiles were orthogonally projected. Sediment density values were constrained from the seismic velocities using the velocity-density relationship [33]. The average density values from adjacent profiles were assigned to the corresponding layer for the profiles without available velocity constraints. At a few locations, deviations from seismic constraints were made when the modeled responses significantly differed from the observed data. Compiled seismic velocities and corresponding densities of different lithospheric bodies are given in Table S3 in supporting information S1. The model output and its fit with the observed data are calculated using Litmod2D v1.6 [34], which solves the heat conduction and geopotential equations to infer the crustal and upper mantle structure.

3.1.1. Calculation of Stretching Factors. We use the modeled Moho and LAB geometries to evaluate the crustal and lithospheric stretching variations along the Red Sea region. The stretching factor for the whole crust (β_C) and the whole lithosphere (β_L) is calculated using the equation [35]

$$\beta = \frac{t_i}{t_f} \tag{1}$$

where t_i is the initial (pre-rift) and t_f is the final (present-day) thickness of the crust and the lithosphere. The pre-rift thickness values were assumed from the average thickness of undisturbed neighboring continental regions. The initial crustal thickness (t_{Ci}) is taken as 43 km, which is the depth to Moho in the Arabian shield as inferred from the deep seismic refraction line of the United States Geological Survey (USGS) [36]. The initial lithospheric thickness (t_{Li}) is assumed to be 120 km for the southern Red Sea and 110 km for the central and northern Red Sea regions, which are the values calculated using receiver function analysis by Hansen et al. [37] for the Arabian shield. To account for the uncertainty of the assumed initial thickness values, β values were calculated for t_{Ci} ± 5 km and t_{Li} ± 10 km. The final thickness values are calculated from the lithospheric models. The difference between the crustal and lithospheric stretching factors ($\beta_C - \beta_L$) was used to analyze the differential stretching of the crust and mantle layers. We prepared the maps of β_C, β_L, and $\beta_C - \beta_L$ for the whole Red Sea region by interpolating the values from the individual profile for a holistic interpretation.

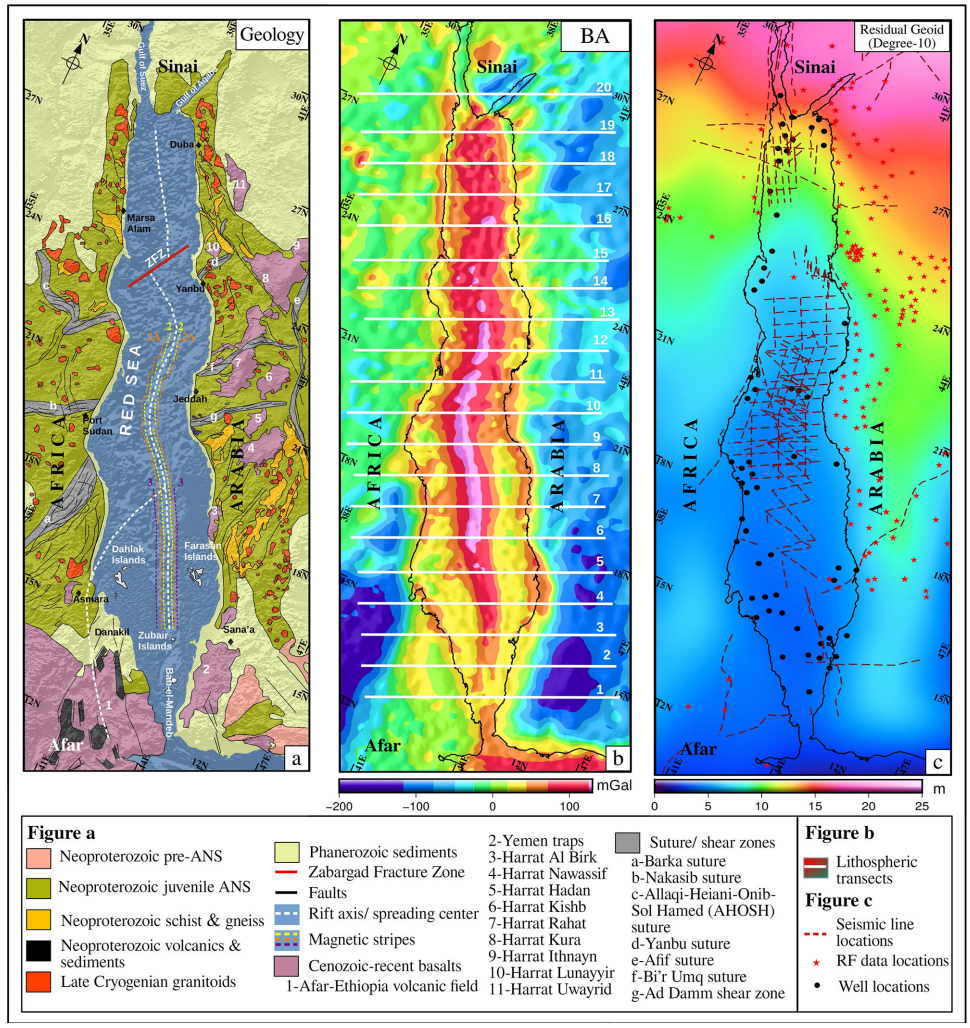

FIGURE 1: (a) Onshore and offshore geology of the Red Sea overlain topography/bathymetry relief, with important tectonic and magmatic features. (b) Bouguer gravity anomaly map of the Red Sea. White lines show profiles used for lithosphere modeling. (c) Degree-10 residual geoid map of the Red Sea with locations of seismic and seismological constraints (see Table S1 in supporting information S1).

3.2. Estimation of Effective Elastic Thickness. Effective elastic thickness (Te) indicates the thickness of a thin elastic plate overlying an inviscid substrate whose response to an applied load is equal to that of a real lithosphere under the same load and is considered a proxy of the integrated strength of the lithosphere [38]. We estimated Te using a joint inversion of admittance and coherence of topography/bathymetry and Bouguer anomaly using the code PlateFlex [39]. In oceanic regions, bathymetry was converted to effective bathymetry to maintain consistency with the offshore Bouguer gravity anomaly by converting the water load to a rock column of average crustal density and adding this column to the bathymetry [40].

3.3. Computation of UMG and RMBA. The gravitational effect of the upper mantle density structure was calculated using the approximate quantitative relationship between density (ρ) and shear wave velocity (Vs) [41] using the equation

$$R_{\frac{\rho}{s}} = \frac{ln\rho - ln\rho_0}{lnV_s - lnV_{s0}} \quad (2)$$

where $R_{\rho/s}$ is the scaling ratio, ρ_0 is the reference density, and V_{s0} is the reference shear wave velocity. We used the shear wave tomography model, as V_s, Global 1-D Earth model ak135-F [42, 43] as ρ_0 and V_{s0}, and the model by Forte et al. [44] for the depth-dependent variation of $R_{\rho/s}$. The modeled density perturbation is converted into the UMG effect using Parker's [45] forward modeling equation.

The mantle Bouguer anomaly (MBA), representing the variations in crustal thickness and crustal and/or mantle density, was computed by correcting the Bouguer anomaly for the crust-mantle interface assuming a reference crust of 6 km thickness and using forward modeling technique [45]. The RMBA is determined by subtracting the UMG from the MBA to remove the effect of deeper density variations, yielding a more accurate representation of crustal-scale density variations.

4. Results

The lithospheric architecture modeled for twenty profiles (Figures 2–6) across the Red Sea region reveals Moho and LAB geometry variations within different basin segments. The calculated values for β_C, β_L, and $\beta_C - \beta_L$ for all twenty profiles are presented in Figure 7. A detailed description of the lithospheric models and stretching factors along the twenty models is given in Text S1 in supporting information (S1). The β_C, β_L, and $\beta_C - \beta_L$ (Figure 8) and Te, UMG, and RMBA maps for the Red Sea region (Figure 9) are analyzed and mutually compared to interpret the links between extension and lithospheric architecture along the Red Sea.

In general, the β_C map (Figure 8(a)) has a close resemblance with the RMBA map (Figure 9(c)). The long, narrow axial zones of β_C (<6) and RMBA (>240 mGal) in the southern and central part of the Red Sea suggest that the most intense crustal thinning coincides with the axial magma chambers of crustal accretion in this region. The β_L (Figure 8(b)) map correlates well with the Te map (Figure 9(a)), indicating that the largest lithospheric stretching is observed in the regions of the weak lithosphere. The identified regions of weak and stretched lithosphere include the Afar Triple Junction (Te = 5 km, β_L ~2.75), the southern Red Sea (Te = 5–10 km, β_L >3), and Zabargad Fracture Zone (ZFZ; Te = 10–15 km, β_L ~2.75). Furthermore, the entire Red Sea region is characterized by negative UMG (Figure 9(b)). A zone of highly negative UMG (<−200 mGal) extends from the Afar region toward the Arabian shield, crossing the southern Red Sea region obliquely (Figure 9(b)).

Based on the variations in these relationships along the basin length, we identify four segments of the Red Sea with distinct geophysical characteristics and use these differences to highlight variations in the extensional style and rifting mechanism.

4.1. Red Sea Segments

4.1.1. Southernmost Red Sea and Danakil. Our models reveal that the southernmost Red Sea and Danakil region are characterized by stretched continental crust and lithosphere (Figure 2) with $\beta_L > \beta_C$ (Figure 6). The calculated β_C values are comparable with previous studies in Afar (~2.0) [46], as well as the Yemen margin (onshore: 1.6–1.8; and offshore: 2.4 [47]). The lack of axial RMBA high suggests the absence of seafloor spreading and substantiates the previous continental rifting interpretations for this segment of the Red Sea [16, 48]. Our models show a domed LAB and magmatically intruded crust in the Danakil region, which can be attributed to the upwelled asthenosphere due to the proximity of the Afar plume [49, 50]. The region of this segment characterized by high β_L (~2.4–2.7) and low Te (<7 km) coincide with a highly negative UMG anomaly (<−200 mGal). We interpret this to indicate the influence of upper mantle density and/or temperature heterogeneities, weakening the lithosphere and promoting elevated lithospheric stretching. Thermal perturbations by mantle plumes can be sufficient to reduce the mechanical strength of the lithosphere [51]. The plume-driven thermal erosion of the lithosphere can decrease the total lithospheric thickness, whereas magma intrusion and underplating increase the crustal thickness [52], yielding elevated β_L and lower β_C values. The results, altogether, suggest mechanical stretching and thinning of the lithosphere in this area which is magmatically affected and thermally weakened by the Afar mantle plume. Our modeling does not consider stretching caused by magma injection [53]

4.1.2. Southern Red Sea. Previous investigations in this region provided evidence of seafloor spreading with an active spreading ridge with magnetic lineations, seismicity, and rift shoulder uplift [5, 16, 54–56]. The RMBA map (Figure 9(c)) shows the presence of a continuous narrow axial high zone. The β_L and Te (figures 8(b) and 9(a)) maps reveal a weak but highly stretched lithosphere centered at the axis of this segment. The lithospheric models (figures 2–4) reveal significant crustal stretching and asymmetry in the Moho and LAB geometry. The Arabian margin is characterized by a thicker oceanic crust, which is related to a combination of downward bowing of the oceanic lithosphere and a relatively thick sedimentary pile overlying the oceanic crust (see also Reference 57). The extent of the oceanic crust is wider in this segment of the Red Sea, extending from the present-day spreading center to the Arabian Escarpment. The Miocene sediments are deposited atop the oceanic crust [57], indicating its earlier formation.

Mafic underplate is modeled at the location of crustal necking beneath the Arabian escarpment (Figure 4), while crustal necking is not evident on the African margin. Upwarping of the LAB is significantly greater on the Arabian margin compared with the southernmost and central Red Sea. Numerical modeling suggests that this lithospheric behavior is promoted by a weaker and/or hotter lithospheric mantle [58]. β_C on the Arabia margin is less than the African margin, which we attribute to the thicker oceanic crust and sediment pile. An asymmetry in lithospheric extension is revealed by the greater extent of elevated β_L values that extend beneath and beyond the Red Sea escarpment beneath the relatively thick crust of the Arabian Shield (β_L ~2.5). In contrast, the African Lithosphere is thicker and undergoes less stretching (β_L ~1.8–2.0; Figure 7). The stretched lithosphere beneath the Arabian margin coincides with a low gravity anomaly zone, as indicated in the UMG map (Figure 9(b)), which extends from the Afar region toward the Arabian shield, crossing the southern Red Sea obliquely.

We interpret these data to reflect the presence of a shallower, buoyant, and presumably hotter sublithospheric mantle beneath the Arabian margin of the southern Red Sea. Upwarping of the LAB promoted thermal erosion at the lithospheric base and higher lithospheric stretching. The coincidence of the thinned lithosphere, mafic underplating, and LAB upwelling beneath the zone of elevated topography along the Arabian escarpment is interpreted to reflect dynamic support from the upper mantle structure [59].

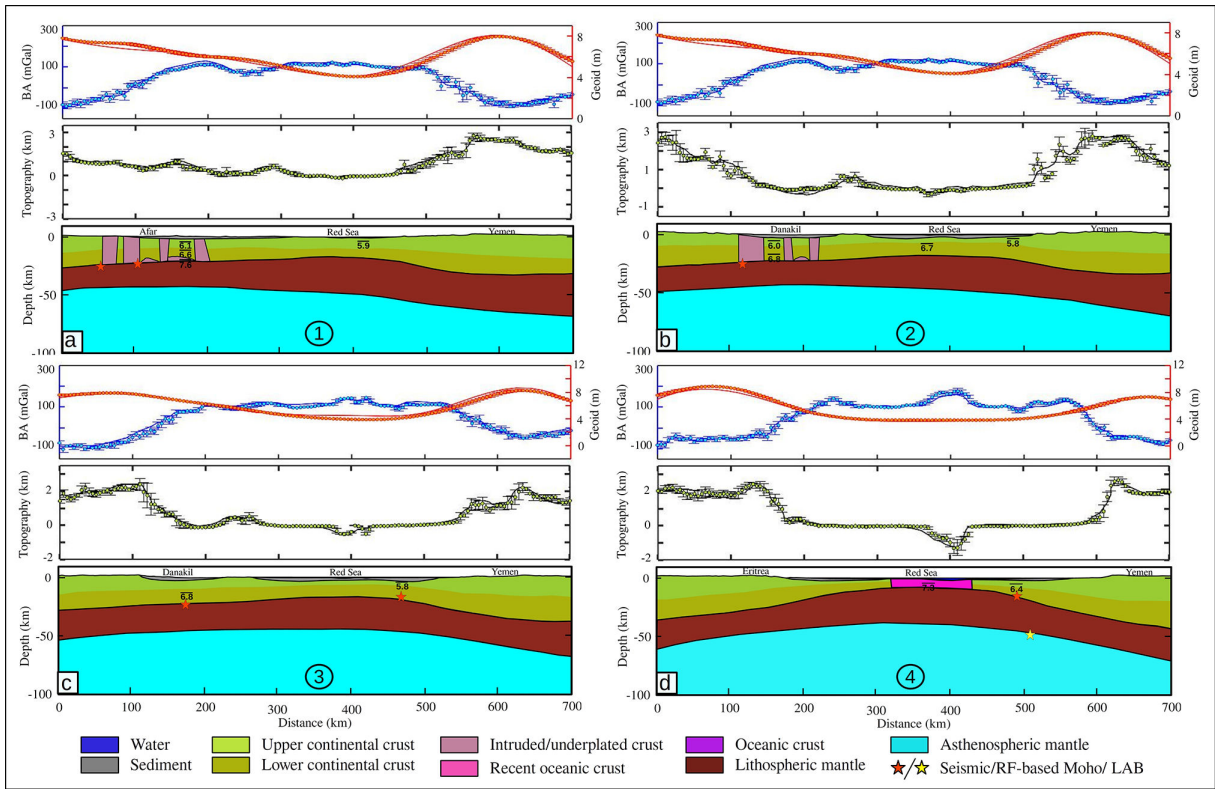

FIGURE 2: Lithospheric models of profiles 1–4.

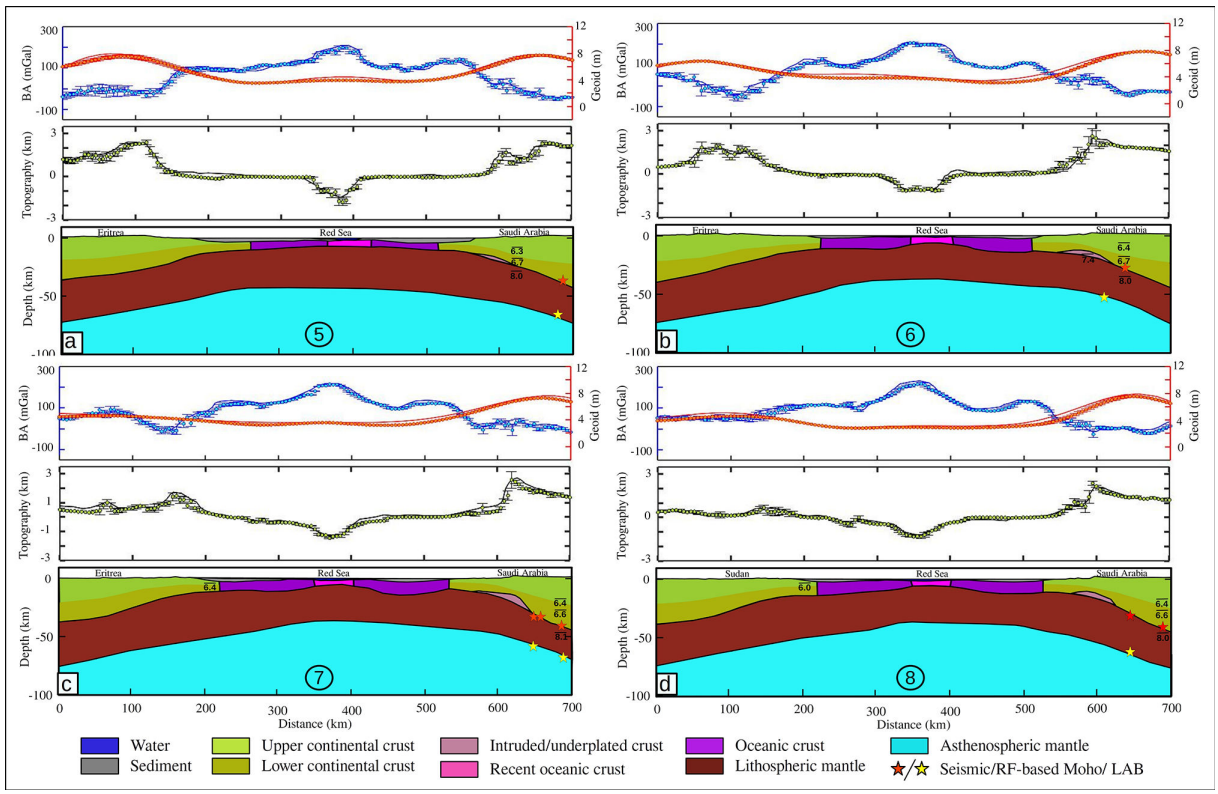

FIGURE 3: Lithospheric models of profiles 5–8.

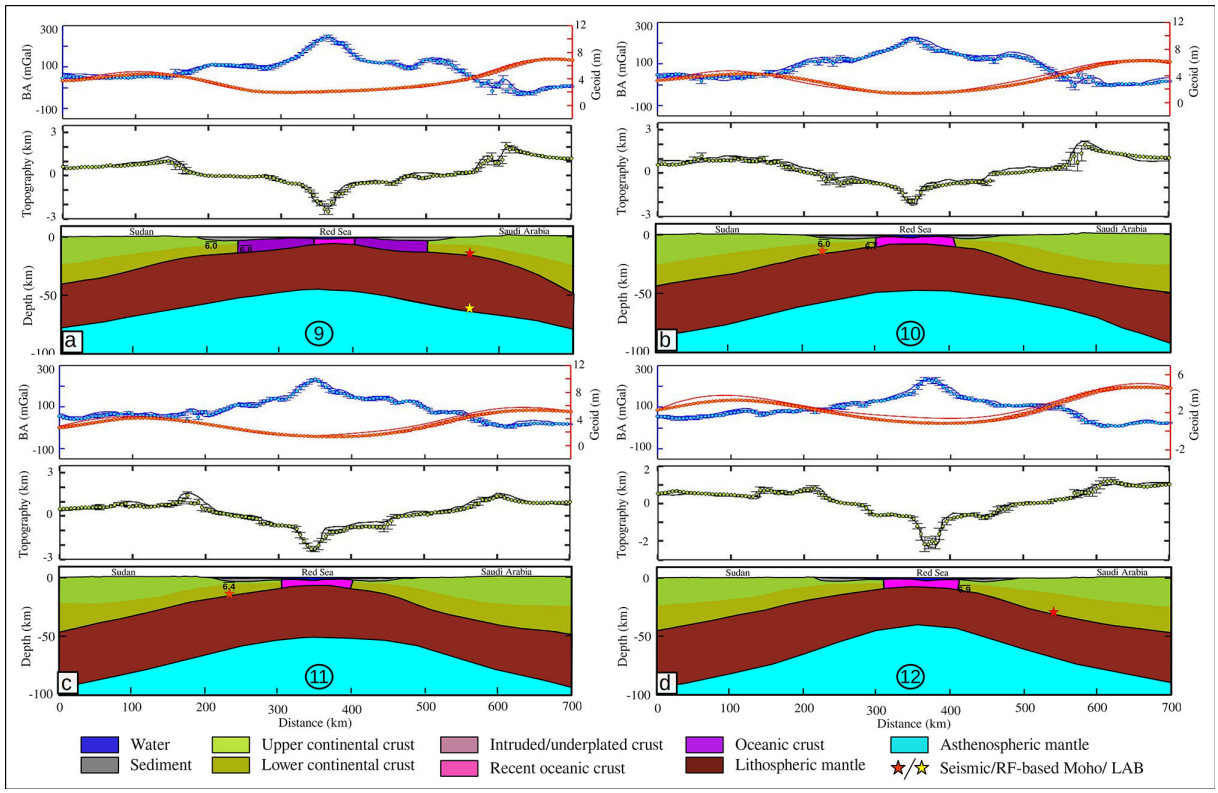

FIGURE 4: Lithospheric models of profiles 9–12.

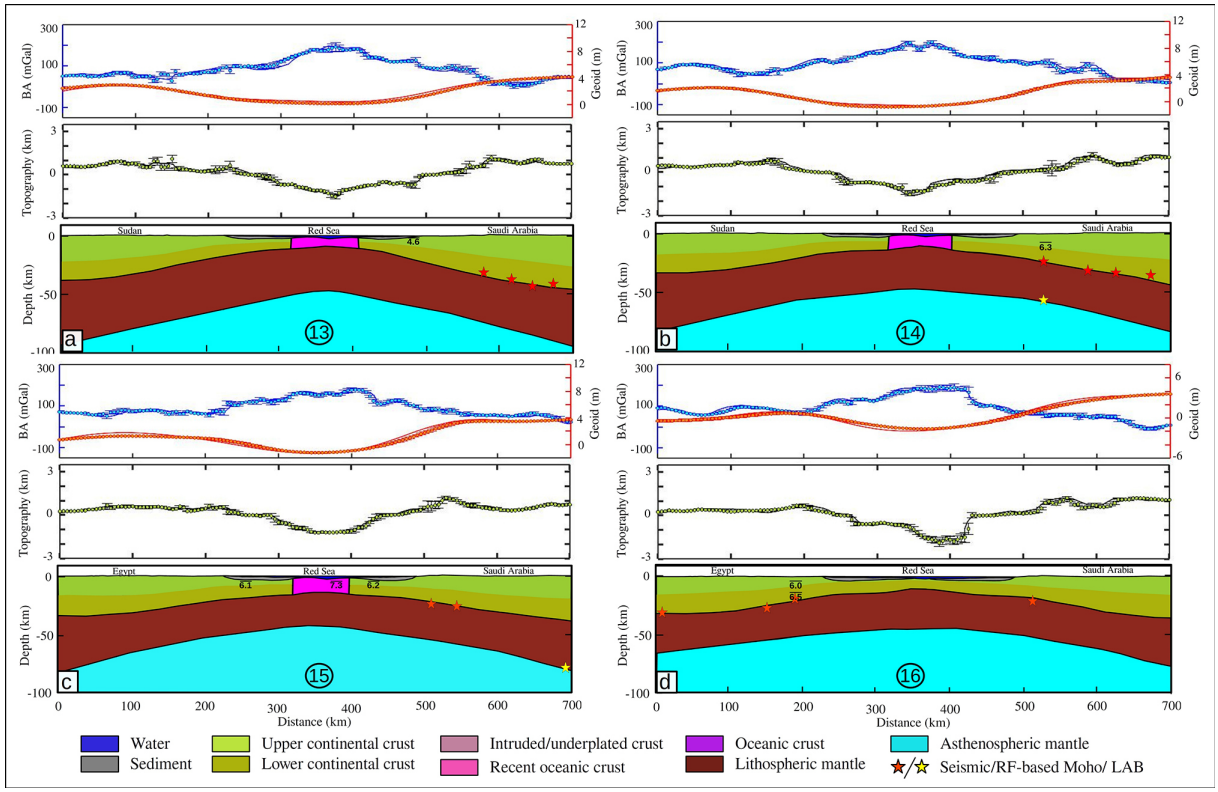

FIGURE 5: Lithospheric models of profiles 13–16.

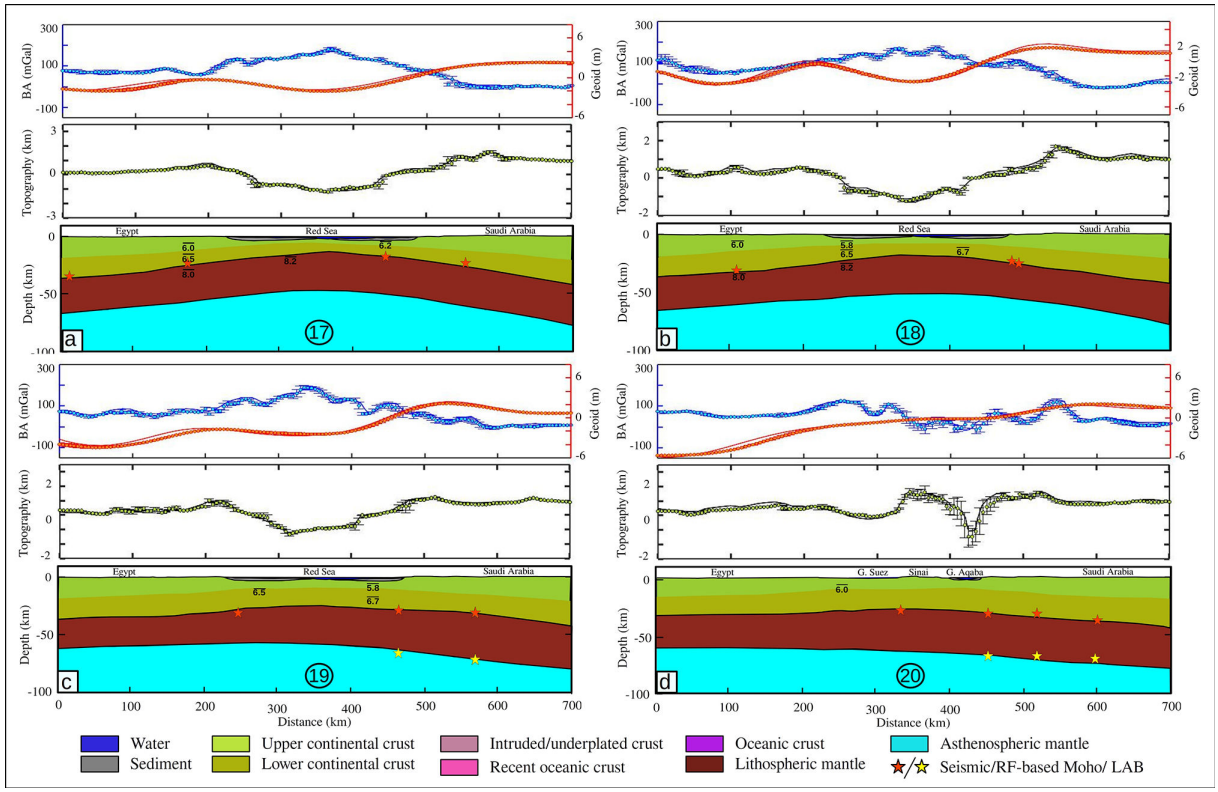

FIGURE 6: Lithospheric models of profiles 17–20.

Thickening of the crust in this domain reflects necking during crustal stretching in combination with intrusion-assisted crustal thickening.

4.1.3. Central Red Sea. The lithospheric models across the central Red Sea (figures 4–5) reveal a narrow axial zone of oceanic crust (or transitional crust) and highly thinned and stretched continental crust flooring overlain by sediments. Unlike the southern Red Sea, the extension of the crust and the lithosphere is relatively symmetrical in this region, suggesting a transition to a pure-shear extension mode. The overall higher crustal stretching (β_C ~5–7) compared with the lithospheric stretching (β_L~2.5; Figure 8) in the basin interior suggests depth-dependent lithospheric stretching [58], in which crustal extension is promoted over lithospheric extension. This type of extension would require decoupling at the crust-mantle interface and increased mantle strength [58]. A strong lithospheric mantle is supported by our moderate Te values (~20 km) for the central Red Sea compared with the Te values from the southern Red Sea. This segment is also characterized by a series of discontinuous axial gravity highs in the RMBA map (Figure 9(c)), which have a similar amplitude and wavelength to anomalies associated with seafloor spreading in the southern Red Sea. The shorter wavelength of mantle upwelling and the geophysical evidence suggest a discontinuous spreading ridge.

4.1.4. Northern Red Sea. The boundary between the central and the northern Red Sea region is defined by the transtensional NE-SW-trending transverse ZFZ (Figure 1). This fracture zone is interpreted as a first-order structure [17] that bounds segments of differential extension between the northern and the central Red Sea [13, 60]. It is expressed by a prominent (~100 km) dextral offset of high amplitude gravity anomalies in the RMBA map (Figure 9(c)) and is also been imaged in compilations of magnetic data [23]. Previous studies have revealed the development of localized pull-apart basins along this structure [23, 60, 61], and it defines the location of the most recently developed "deep" along the axial zone of the central Red Sea [20]. Our Te map reveals a low elastic thickness (~10 km) adjacent to the ZFZ compared with regions to the north and south, highlighting a localized zone of lithospheric weakness (Figure 8(a)). This weak lithosphere is also characterized by increased lithospheric stretching compared with the central Red Sea and regions to the north (Figure 8(b)).

Numerous previous studies suggest that the northern Red Sea is characterized by continental rifting [9], significant extension and thinning of the continental crust, limited formation of new oceanic crust [62–64], and no magnetic evidence for a linear spreading ridge [19]. This contrasts with some recent studies [17, 23, 65, 66] which propose continuous spreading along the entire Red Sea based on gravity data. The lithospheric models in this segment (Figure 6) reveal the presence of continental crust with reduced crustal (β_C ~2) and lithospheric (β_L ~2) stretching. The similarities between β_C and β_L suggest a relatively strong coupling between the crust and upper mantle compared with the remainder of the Red Sea. The

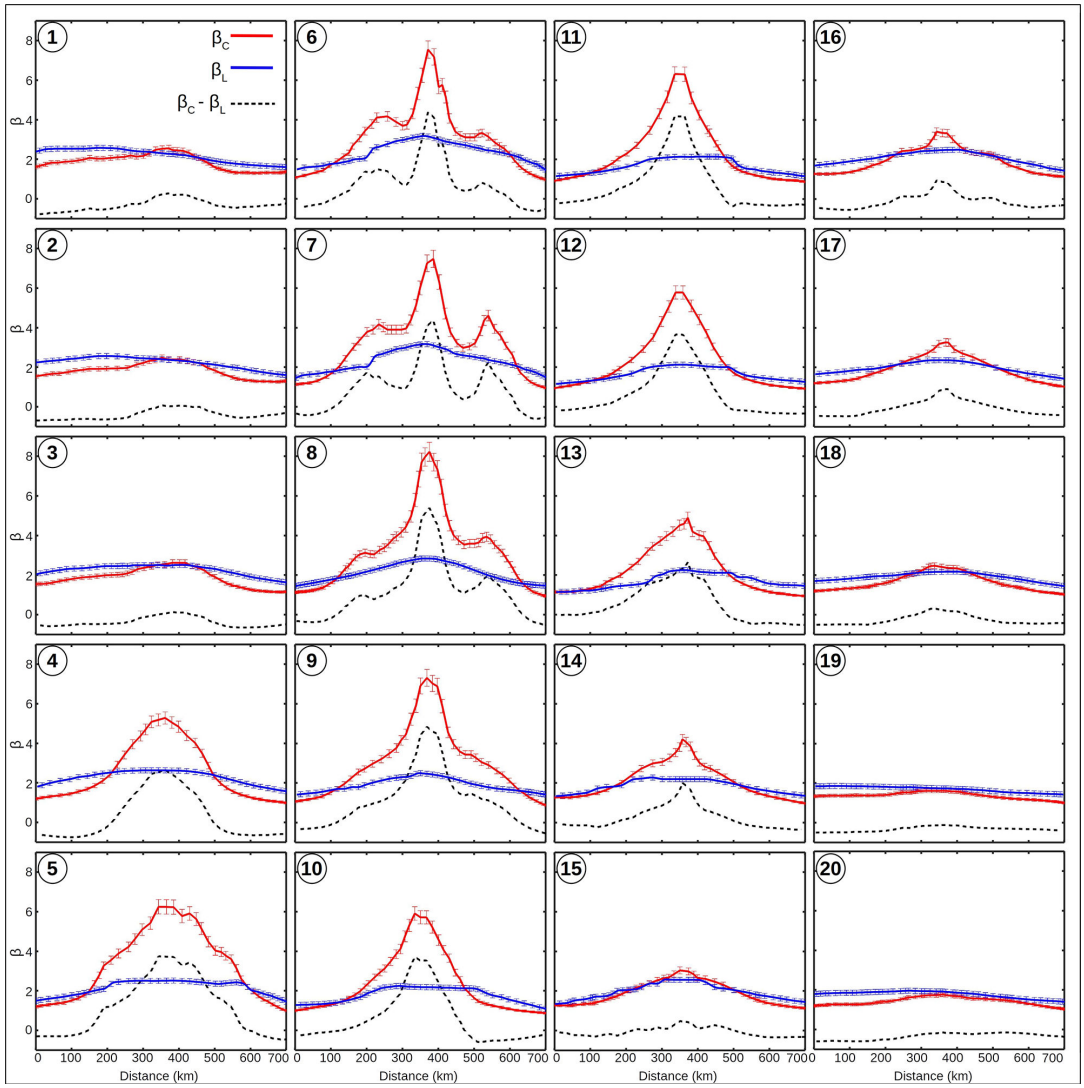

Figure 7: Stretching factor variations along twenty profiles.

axial spreading ridge, which was evident from the RMBA map (Figure 9(c)) in the southern and central Red Sea, is absent in the northern Red Sea. The modeled Moho and LAB geometries suggest pure-shear lithospheric extension, which is generally supported by the β_C and β_L maps (Figure 8), which shows a slight increase in the stretching factor in the center of the basin. This interpretation is consistent with numerous previous studies [15, 63, 67]. The northern Red Sea shows higher (>30 km) Te values (Figure 9(a)) indicating the presence of a mechanically stronger and cooler lithosphere in this region, which is supported by the reduced heat flow compared with the southern part of the Red Sea [68], and the high amplitude UMG anomalies along this northern segment (Figure 9(b)). We note that the northernmost part of this segment (profiles 19 and 20 in Figure 7) shows a minor asymmetry with higher lithospheric extension along the African margin compared with the Arabian Margin, while β_C remains to be symmetric. This relationship is attributed to asymmetric extension along the Gulf of Suez [67, 69].

5. Discussion

The Red Sea represents the modern archetype of evolving juvenile rift systems and offers critical insights into how continental rifts evolve into ocean basins. There have been many different models proposed to explain the evolution and the lithospheric architecture of the Red Sea, and debate continues about the role of the Afar plume versus far-field forces (see Reference 22), the timing and extent of seafloor spreading [5, 16, 17, 54, 55, 55, 56, 70–74], and the mode of crustal extension (i.e., pure shear versus simple shear versus strike-slip) [11, 55, 75–79]. The variability in evolutionary models is often a consequence of

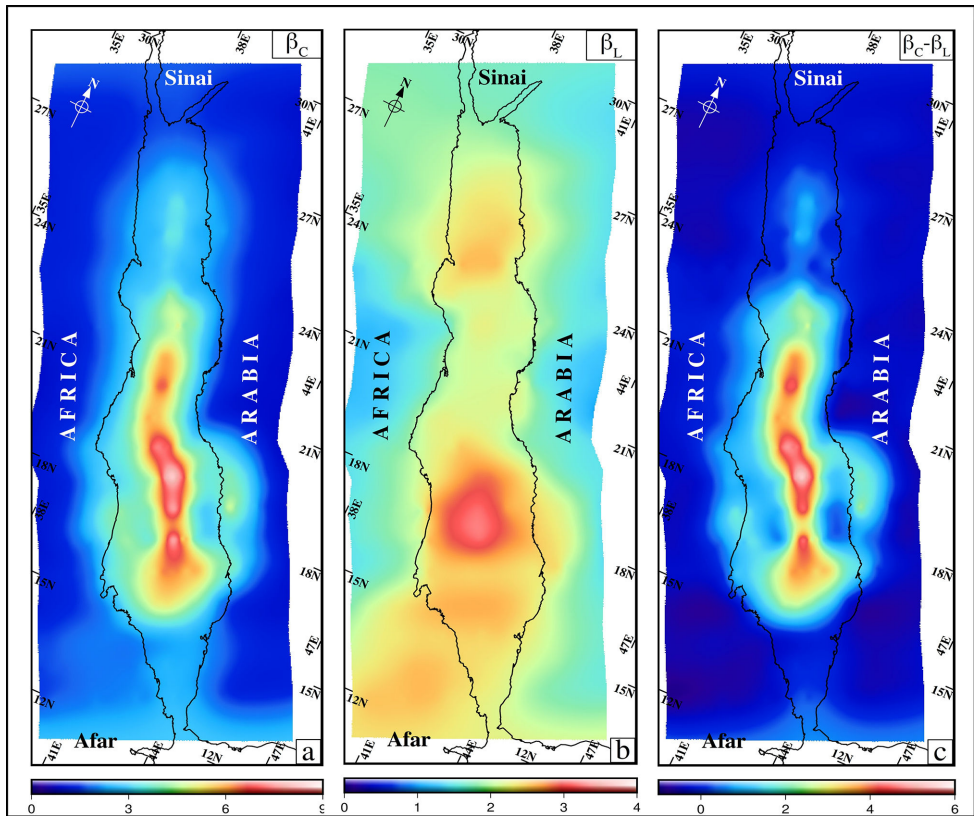

FIGURE 8: Maps of (a) β_C , (b) β_L , and (c) $\beta_C - \beta_L$ of the Red Sea.

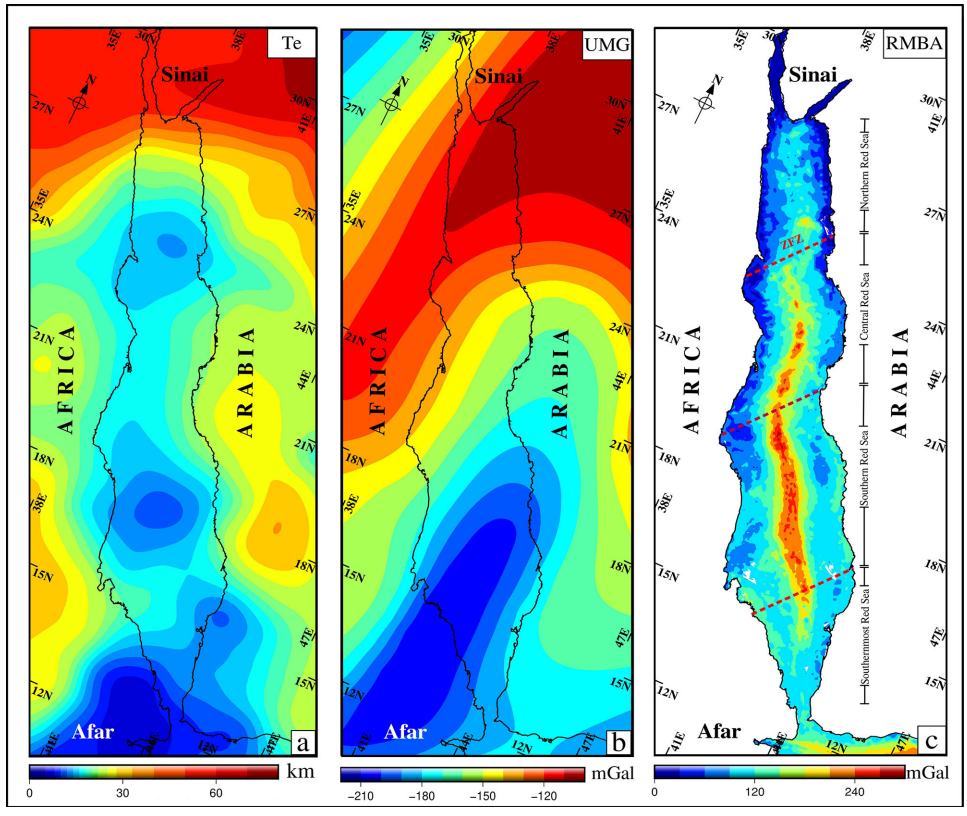

FIGURE 9: Maps of (a) Te, (b) UMG, and (c) RMBA of the Red Sea. Location of the segment boundaries is shown as dashed lines in (c).

interpretations from relatively localized and shallow crustal data that then proliferated along the entire length of the Red Sea. Our approach investigates the lithospheric-scale structure of the entire length of the Red Sea and uses data from multiple and independent data sets to inform our analysis and interpretation.

Our analysis reveals that the Red Sea is highly segmented at both a crustal and lithospheric scale and does neither support the notion that the seafloor spreading is continuous along the axial zone nor that the Red Sea is completely floored by oceanic crust. This substantiates earlier interpretations of discrete spreading segments from geophysical data [16, 80] as well as numerical and analog experiments [81, 82]. We have identified four distinct segments of the Red Sea, each with a distinct lithospheric architecture, which can be correlated with the elastic thickness and subcrustal lithospheric mantle structure. Primary observations regarding the lithospheric structure and extensional styles of these four segments are summarized in Figure 10. The southernmost and northern Red Sea has not yet evolved into active spreading. Both areas have comparable β_C and β_L values (~1.5–2), indicating a state of mechanical coupling during the stretching of the crust and lithospheric mantle. However, the zone of lithospheric extension is significantly wider in the southernmost Red Sea compared with the northern segment (Figure 8). This may be explained by the relatively weak and hot buoyant lithosphere, which is conducive to conditions that favor wide rift modes [83]. In contrast, the relatively strong and cool lithosphere in the northern Red Sea favors narrow rifting [83]. Additionally, the models indicate a significant presence of magmatic intrusion in the Danakil region, which could potentially be a contributing factor to the lithospheric extension [84, 85] and lithospheric weakening [86–88].

Our models show the presence of thick sediment deposits throughout the entire Red Sea. In the northern Red Sea, a continuous salt layer is present between the coastlines. In the central Red Sea, sedimentary deposits are thick and cover the stretched continental crust underlying most of the basin, with narrow axial troughs lacking significant salt deposits. In the southern Red Sea, thick sediment deposits are found along the margins and partially overlie the wide oceanic crust. The results are consistent with various drilling [1–3] and seismic studies [4–8] and other sources listed in Table S1, which revealed extensive sedimentary layers, some up to 4 km thick, dating from the Early Miocene to the Pleistocene period.

A wide zone of oceanic crust underlies the southern Red Sea compared with the rest of the Red Sea, which is partially overlain by Miocene sediments. Almalki et al. [57] attributed this to an episode of Oligocene spreading followed by a spreading hiatus and then renewed Pliocene spreading initiation. Alternatively, it may reflect continuous spreading since the Miocene, as proposed by Augustin et al. [17]. Regardless of the preferred interpretation, the oceanic crust is more extensive in the southern segment than in the central Red Sea (see also Reference 16). The continuity in the axial seafloor spreading is evident in the β_C and RMBA maps (figures 8(a) and 9(c)). Variations in the β_C and β_L values in the southern Red Sea suggest a decoupling of the crust and lithospheric mantle. Crustal extension in the axial zone is more than twice that of the lithosphere, suggesting that lithospheric extension may have been accommodated by magma intrusion [89]. β_L is more diffuse with maximum stretching in the central part of the segment and tapers off more moderately on the Arabian margin compared with the African margin (Figure 8(b)), revealing an asymmetry that is further evidenced by crustal necking, underplating (Figure 3), and topographic uplift along the Arabian Escarpment [90]. The coincidence of maximum lithospheric extension and a significant Te low in the central part of the segment points to lithospheric strength as a major control on the seafloor spreading. The UMG map shows this part of the Red Sea is obliquely intersected with an elongated regional low (−200 mGal), which may be imaging a low-density mantle channel [91–93] that extends from the Afar mantle plume across the southern Red Sea. This may be conducive to the post-rift evolution of the elevated Arabian margin [94] and the formation of a chain of volcanic fields (Harrats) in the Arabian shield as the surface expression of decompression melting of the plume channel [95]. This is further supported by low velocities beneath the Arabian escarpment in the global [30] and local tomography models [96].

There are some similarities between the central and the southern Red Sea segments, particularly in terms of the crustal extension along the axial zone, which is significant, although slightly less. The RMBA response in the central segment is also similar in wavelength and amplitude to the southern segment, but the anomalies are less continuous. A decoupling of crust and lithospheric mantle is still apparent in the β_C and β_L values, suggesting magma intrusion-assisted lithospheric extension. These findings are consistent with the depth-dependent extension model [97, 98] which suggests that the decoupling of the lithosphere leads to crustal-necking breakup following the lithospheric-mantle necking breakup. The Red Sea break-up model, as presented by Mohriak and Leroy [99], which suggests a rapid thinning of the continental crust from onshore to offshore and the initiation of spreading in the axial trough, thereby separating two Late Miocene salt basins, aligns well with this interpretation. The central Red Sea is symmetrical in comparison to the southern Red Sea, and the oceanic crust is significantly narrower, suggesting that this segment is more juvenile. This is supported by interpretations of localized upwelling mantle diapirs impingement, emplaced oceanic crust, and development of isolated bathymetric deeps along the axial zone [18, 20, 21, 73] and marked change in the signal of marine and satellite magnetic anomalies away from the axial zone [16, 23]. The Te map suggests that the lithosphere is stronger and less stretched beneath this segment compared with the southern Red Sea segment, which highlights the diminishing influence of the

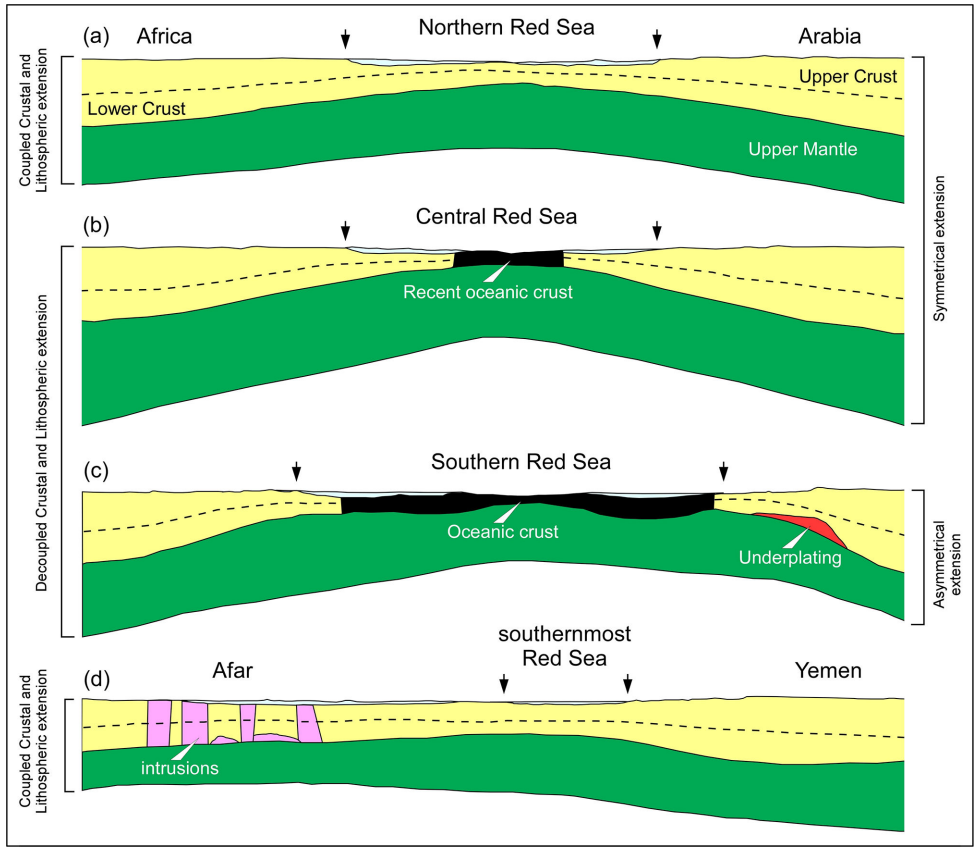

FIGURE 10: Illustrative summary of the lithospheric structure and extensional styles of the four Red Sea segments. Dashed lines indicate representative boundaries between the upper and lower continental crusts.

Afar mantle plume. The narrowness of mantle upwelling in this section compared with the southern Red Sea could be attributed either to the immaturity of the spreading compared with the south, or the relatively high strength of the lithosphere, noting this condition would promote narrow rifting [83]. In either case, the present results support earlier observations of a transition zone in the central Red Sea [10, 16, 19, 73].

An intriguing observation along the axis of the Red Sea is the coincidence between the first-order ZFZ [17] at the boundary between the central and northern segments. In the upper crust, the ZFZ is revealed as offsets in the RMBA. However, the fracture zone is also imaged in the β_L map and is defined in the Te map as a significant low. These observations suggest that the ZFZ is a lithospheric scale boundary that has locally weakened the lithosphere and imparts significant control of lithospheric stretching and rifting. The ZFZ also coincides with the terrane bounding AHOSH - Yanbu sutures (Figure 1(a)) [100], and inherited lithospheric rheology contrasts across this suture may have imparted control on the mode of extension between the central and northern Red Sea segments. This boundary may be a barrier to seafloor spreading propagation, as evidenced by numerous rotational rifting analog experiments with deep-seated heterogeneities [101]. This zone of the weak lithosphere and higher lithospheric extension may be recording the onset of a new oceanic spreading cell with different characteristics to the central Red Sea.

Overall, our analysis suggests that the Red Sea has not evolved by simply "unzipping" due to the rotation of Arabia with respect to Africa which was suggested by previous kinematic models [54, 102]. Rather, the origin of this young ocean basin is complex, with both the far-field tectonic forces and the Afar mantle plume having a significant effect by promoting a wide rift mode of extension, strong decoupling of the upper mantle and crust, and commensurate asymmetric lithospheric geometry.

6. Conclusions

The residual gravity anomalies, along with the derived lithospheric structure and rheology along the Red Sea region, reveal varying styles of lithospheric extension along the Red Sea. Based on the lithospheric architecture and extensional styles, four distinct segments are suggested.

The segment comprising the southernmost Red Sea and Danakil region is characterized by a hot, weak, and stretched lithosphere. The extension within the Danakil region shows the characteristics of the lithosphere which is highly influenced by the Afar mantle plume.

The southern Red Sea is revealed as a region of a continuous spreading ridge and a wider zone of

oceanic crust. Our results reveal a weaker lithosphere with significant crustal stretching β_C and differential stretching between the crust and lithospheric mantle. The Arabian side of the margin reveals a thicker crust with underplating material and up-warped LAB with higher lithospheric stretching. We attribute this asymmetric extension to the sublithospheric channeling of the Afar mantle plume.

The central Red Sea is stretching in a pure-shear mode with moderately depth-dependent stretching. This segment is characterized by an axial region of discontinuous emplacement of oceanic crust and may represent a less mature spreading center compared with the southern Red Sea. The influence of the Afar mantle plume is minimal in this segment compared with the southern Red Sea.

The northern Red Sea's lithosphere is stronger, colder, and less stretched than other Red Sea segments, exhibiting characteristics consistent with a continental rift. Additionally, the crust and lithospheric mantle have comparable amounts of stretching, indicating mechanical coupling between these layers during the process.

The ZFZ bounding the central and northern Red Sea region is a significant lithospheric boundary with a weak and stretched lithosphere, which may be acting as a barrier to seafloor spreading propagation toward the north. Furthermore, this zone may be recording the onset of a future oceanic spreading cell with different characteristics to the central Red Sea.

The varying lithospheric architecture and extensional styles within the Red Sea segments suggest that the opening of this nascent ocean basin is not due to a simple "unzipping" caused by the rotation of the Arabian plate but evolved in a more complex setting influenced by both the Afar mantle plume, far-field tectonic forces, and rheological variations.

Data Availability

ETOPO1 global relief model is available at https://www.ngdc.noaa.gov/mgg/global/. Free-air gravity grid is available at https://topex.ucsd.edu/cgi-bin/get_data.cgi/. EGM2008 geoid grid is available at http://icgem.gfz-potsdam.de/home/. Tomography model SL2013sv is available at https://schaeffer.ca/tomography/sl2013sv/.

Conflicts of Interest

The authors declare that there is no conflict of interest regarding the publication of this paper.

Acknowledgments

The authors thank the IITB-Monash Research Academy for facilitating this research work. This research work forms part of the Ph.D. research of the first author (K. S. Sreenidhi) which was financially supported by the IITB-Monash Research Academy.

Supplementary Materials

The supplementary file contains three supplementary tables (S1-S3) and a supplementary text (S1). Table S1 includes the sources of various seismic, seismological, and well constraints used in the modeling. Table S2 contains average density, thermal conductivity, and volumetric heat production values assumed for various lithospheric bodies during computation. Table S3 contains the compiled seismic velocities and corresponding densities of different lithospheric bodies used in the modeling. Supplementary text S1 provides a detailed description of the lithospheric models and stretching factors along twenty profiles.

References

[1] Z. R. Beydoun and A. H. Sikander, "The red sea—Gulf of Aden: re-assessment of hydrocarbon potential," *Marine and Petroleum Geology*, vol. 9, no. 5, pp. 474–485, 1992.

[2] G. W. Hughes and Z. R. Beydoun, "The red sea—Gulf of Aden: Biostratigraphy, Lithostratigraphy and Palaeoenvironments," *Journal of Petroleum Geology*, vol. 15, no. s3, pp. 135–156, 1992. https://onlinelibrary.wiley.com/toc/17475457/15/s3.

[3] A. Y. Izzeldin, "Seismic, gravity and magnetic surveys in the central part of the Red sea: their interpretation and implications for the structure and evolution of the Red sea," *Tectonophysics*, vol. 143, no. 4, pp. 269–306, 1987.

[4] P. Skipwith, *The Red Sea and Coastal Plain of the Kingdom of Saudi Arabia: A Review*, Ministry of Petroleum and Mineral Resources, Deputy Ministry for Mineral Resources, 1973.

[5] R. W. Girdler and P. Styles, "Two stage Red sea floor spreading," *Nature*, vol. 247, no. 5435, pp. 7–11, 1974.

[6] D. Davies and C. Tramontini, "A discussion on the structure and evolution of the Red sea and the nature of the Red sea, Gulf of Aden and Ethiopia rift junction-the deep structure of the Red sea," *Philosophical Transactions of the Royal Society of London. Series A, Mathematical and Physical Sciences*, vol. 267, no. 1181, pp. 181–189, 1970.

[7] F. Egloff, R. Rihm, J. Makris, et al., "Contrasting structural styles of the Eastern and Western margins of the Southern Red sea: the 1988 SONNE experiment," *Tectonophysics*, vol. 198, nos. 2–4, pp. 329–353, 1991.

[8] D. A. Ross and J. Schlee, "Shallow structure and geologic development of the Southern Red sea," *Geological Society of America Bulletin*, vol. 84, no. 12, 1973.

[9] J. R. Cochran and G. D. Karner, "Constraints on the deformation and rupturing of Continental Lithosphere of the Red sea: the transition from Rifting to drifting," *Geological Society, London, Special Publications*, vol. 282, no. 1, pp. 265–289, 2007.

[10] K. A. Almalki, P. G. Betts, and L. Ailleres, "The red Sea–50 years of geological and geophysical research," *Earth-Science Reviews*, vol. 147, pp. 109–140, 2015.

[11] J. Makris and R. Rihm, "Shear-controlled evolution of the Red sea: pull apart model," *Tectonophysics*, vol. 198, nos. 2–4, pp. 441–466, 1991.

[12] R. G. Bohannon, "Style of Extensional Tectonism during Rifting, red sea and Gulf of Aden," *Journal of African Earth*

Sciences (and the Middle East), vol. 8, nos. 2–4, pp. 589–602, 1989.

[13] T. H. Dixon, E. R. Ivins, and B. J. Franklin, "Topographic and volcanic asymmetry around the Red sea: constraints on rift models," *Tectonics*, vol. 8, no. 6, pp. 1193–1216, 1989.

[14] W. Voggenreiter and H. Hötzl, "Kinematic evolution of the Southwestern Arabian Continental margin: implications for the origin of the Red sea," *Journal of African Earth Sciences (and the Middle East)*, vol. 8, nos. 2–4, pp. 541–564, 1989.

[15] A. Hosny and A. Nyblade, "Crustal structure in southeastern Egypt: symmetric thinning of the northern Red sea Rifted margins," *Geology*, vol. 42, no. 3, pp. 219–222, 2014.

[16] K. A. Almalki, P. G. Betts, and L. Ailleres, "Incipient Seafloor spreading segments: insights from the Red sea," *Geophysical Research Letters*, vol. 43, no. 6, pp. 2709–2715, 2016. https://agupubs.onlinelibrary.wiley.com/toc/19448007/43/6.

[17] N. Augustin, F. M. van der Zwan, C. W. Devey, and B. Brandsdóttir, "13 million years of Seafloor spreading throughout the Red sea Basin," *Nature Communications*, vol. 12, no. 1, 2021.

[18] E. Bonatti, A. Cipriani, and L. Lupi, "The red sea: birth of an ocean," in *The Red Sea*, pp. 29–44, Springer, Berlin, Heidelberg, 2015.

[19] S. El Khrepy, I. Koulakov, T. Gerya, N. Al-Arifi, M. S. Alajmi, and A. N. Qadrouh, "Transition from Continental Rifting to Oceanic spreading in the northern Red sea area," *Scientific Reports*, vol. 11, no. 1, 2021.

[20] M. Ligi, E. Bonatti, F. C. Tontini, et al., "Initial burst of Oceanic crust accretion in the Red sea due to edge-driven Mantle convection," *Geology*, vol. 39, no. 11, pp. 1019–1022, 2011.

[21] N. C. Mitchell and Y. Park, "Nature of crust in the central Red sea," *Tectonophysics*, vol. 628, pp. 123–139, 2014.

[22] T. Z. Aldaajani, K. A. Almalki, and P. G. Betts, "Plume versus slab-pull: example from the Arabian plate," *Frontiers in Earth Science*, vol. 9, p. 700550, 2021.

[23] R. Issachar, J. Ebbing, and Y. Dilixiati, "New magnetic anomaly map for the Red sea reveals Transtensional structures associated with Rotational Rifting," *Scientific Reports*, vol. 12, no. 1, 2022.

[24] N. Molnar, A. Cruden, and P. Betts, "The role of inherited Crustal and Lithospheric architecture during the evolution of the Red sea: insights from three dimensional analogue experiments," *Earth and Planetary Science Letters*, vol. 544, 2020.

[25] R. J. Stern and P. R. Johnson, "Constraining the opening of the Red sea: evidence from the Neoproterozoic margins and Cenozoic Magmatism for a volcanic Rifted margin," in *In Geological setting, palaeoenvironment and archaeology of the Red Sea*, pp. 53–79, Springer, Cham, 2019.

[26] C. Amante and B. W. Eakins, *ETOPO1 Arc-Minute Global Relief Model: Procedures, Data Sources and Analysis*, 2009.

[27] D. T. Sandwell, R. D. Müller, W. H. F. Smith, E. Garcia, and R. Francis, "New global marine gravity model from Cryosat-2 and Jason-1 reveals buried Tectonic structure," *Science (New York, N.Y.)*, vol. 346, no. 6205, pp. 65–67, 2014.

[28] N. K. Pavlis, S. A. Holmes, S. C. Kenyon, and J. K. Factor, "The development and evaluation of the earth gravitational model 2008 (Egm2008)," *Journal of Geophysical Research*, vol. 117, no. B4, 2012.

[29] G. S. Rao and M. Radhakrishna, "India-Elan Bank-East Antarctica breakup, Crustal architecture, and margin evolution: results from constrained potential field and Process-Oriented gravity modeling of conjugate margin segments," *Tectonics*, vol. 40, no. 2, 2021.

[30] A. J. Schaeffer and S. Lebedev, "Global shear speed structure of the upper Mantle and transition zone," *Geophysical Journal International*, vol. 194, no. 1, pp. 417–449, 2013.

[31] H. Zeyen, P. Ayarza, M. Fernàndez, and A. Rimi, "Lithospheric structure under the Western African-European plate boundary: A Transect across the Atlas mountains and the Gulf of Cadiz," *Tectonics*, vol. 24, no. 2, 2005.

[32] C. E. Keen and S. A. Dehler, "Extensional styles and gravity anomalies at Rifted Continental margins: some North Atlantic examples," *Tectonics*, vol. 16, no. 5, pp. 744–754, 1997.

[33] J. E. Nafe and C. L. Drake, "Variation with depth in shallow and deep water marine sediments of porosity, density and the velocities of Compressional and shear waves," *GEOPHYSICS*, vol. 22, no. 3, pp. 523–552, 1957.

[34] J. C. Afonso, M. Fernàndez, G. Ranalli, W. L. Griffin, and J. A. D. Connolly, "Integrated geophysical-Petrological modeling of the Lithosphere and Sublithospheric upper Mantle," *Geochemistry, Geophysics, Geosystems*, vol. 9, no. 5, 2008.

[35] D. McKenzie, "Some remarks on the development of sedimentary basins," *Earth and Planetary Science Letters*, vol. 40, no. 1, pp. 25–32, 1978.

[36] W. D. Mooney, M. E. Gettings, H. R. Blank, and J. H. Healy, "Saudi Arabian seismic-refraction profile: a Traveltime interpretation of Crustal and upper Mantle structure," *Tectonophysics*, vol. 111, nos. 3–4, pp. 173–246, 1985.

[37] S. E. Hansen, A. J. Rodgers, S. Y. Schwartz, and A. M. S. Al-Amri, "Imaging ruptured Lithosphere beneath the Red sea and Arabian Peninsula," *Earth and Planetary Science Letters*, vol. 259, nos. 3–4, pp. 256–265, 2007.

[38] A. B. Watts, *Isostasy and Flexure of the Lithosphere*, Cambridge University Press, 2001.

[39] P. Audet, "Plateflex: software for mapping the elastic thickness of the Lithosphere (version V0.1.0). Zenodo," , 2019. https://doi.org/10.5281/zenodo.3576803.

[40] C. P. Stark, "Wavelet transform mapping of effective elastic thickness and plate loading: validation using synthetic data and application to the study of Southern African Tectonics," *Journal of Geophysical Research*, vol. 108, no. B12, 2003.

[41] D. G. Isaak, O. L. Anderson, T. Goto, and I. Suzuki, "Elasticity of single-crystal Forsterite measured to 1700K," *Journal of Geophysical Research*, vol. 94, no. B5, pp. 5895–5906, 1989.

[42] B. L. N. Kennett, E. R. Engdahl, and R. Buland, "Constraints on seismic velocities in the earth from Traveltimes," *Geophysical Journal International*, vol. 122, no. 1, pp. 108–124, 1995.

[43] J. P. Montagner and B. L. N. Kennett, "How to reconcile body-wave and normal-mode reference earth models," *Geophysical Journal International*, vol. 125, no. 1, pp. 229–248, 1996.

[44] A. M. Forte, R. L. Woodward, and A. M. Dziewonski, "Joint Inversions of seismic and Geodynamic data for models of Three- dimensional Mantle heterogeneity," *Journal of Geophysical Research*, vol. 99, 1994.

[45] R. L. Parker, "The rapid calculation of potential anomalies," *Geophysical Journal International*, vol. 31, no. 4, pp. 447–455, 1973.

[46] D. J. Ferguson, J. Maclennan, I. D. Bastow, et al., "Melting during late-stage Rifting in afar is hot and deep," *Nature*, vol. 499, no. 7456, pp. 70–73, 2013.

[47] A. Ayele, D. Keir, C. Ebinger, et al., "September 2005 Mega-Dike Emplacement in the Manda-Harraro nascent Oceanic rift (afar depression)," *Geophysical Research Letters*, vol. 36, no. 20, 2009.

[48] I. A. N. Davison, M. Al-kadasi, S. Al-khirbash, et al., "Geological evolution of the southeastern Red sea rift margin, Republic of Yemen," *Geological Society of America Bulletin*, vol. 106, no. 11, pp. 1474–1493, 1994.

[49] C. J. Ebinger, T. D. Bechtel, D. W. Forsyth, and C. O. Bowin, "Effective elastic plate thickness beneath the East African and afar plateaus and dynamic compensation of the Uplifts," *Journal of Geophysical Research*, vol. 94, no. B3, pp. 2883–2901, 1989.

[50] C. Hofmann, V. Courtillot, G. Féraud, et al., "Timing of the Ethiopian flood Basalt event and implications for plume birth and Globalchange," *Nature*, vol. 389, no. 6653, pp. 838–841, 1997.

[51] R. T. Ratheesh Kumar and B. F. Windley, "Spatial variations of effective elastic thickness over the Ninetyeast ridge and implications for its structure and Tectonic evolution," *Tectonophysics*, vol. 608, pp. 847–856, 2013.

[52] M. Stab, N. Bellahsen, R. Pik, X. Quidelleur, D. Ayalew, and S. Leroy, "Modes of Rifting in Magma-Rich settings: Tectono-Magmatic evolution of central afar," *Tectonics*, vol. 35, no. 1, pp. 2–38, 2016.

[53] W. R. Buck, "The role of Magma in the development of the Afro-Arabian rift system," *Geological Society, London, Special Publications*, vol. 259, no. 1, pp. 43–54, 2006.

[54] W. Bosworth, "The red sea and Gulf of Aden basins. In: Catuneanu O, Guiraud R, Erikssonp, Thomas B, shone R, key R(Eds) Phanerozoic evolution of Africa," *Journal of African Earth Sciences (Oxford, England: 1994)*, vol. 43, pp. 334–378, 2005.

[55] R. C. James, "A model for development of the Red sea," *AAPG Bulletin*, vol. 67, pp. 41–69, 1983.

[56] R. C. Searle and D. A. Ross, "A geophysical study of the Red sea axial trough between 20 5° and 22° N," *Geophysical Journal International*, vol. 43, no. 2, pp. 555–572, 1975.

[57] K. A. Almalki, P. G. Betts, and L. Ailleres, "Episodic sea-floor spreading in the Southern Red sea," *Tectonophysics*, vol. 617, pp. 140–149, 2014.

[58] A. E. Svartman Dias, N. W. Hayman, and L. L. Lavier, "Thinning factor distributions viewed through numerical models of Continental extension," *Tectonics*, vol. 35, no. 12, pp. 3050–3069, 2016.

[59] A. Daradich, J. X. Mitrovica, R. N. Pysklywec, S. D. Willett, and A. M. Forte, "Mantle flow, dynamic topography, and rift-flank uplift of Arabia," *Geology*, vol. 31, no. 10, 2003.

[60] K. Crane and E. Bonatti, "The role of fracture zones during early Red sea Rifting: structural analysis using space shuttle radar and LANDSAT imagery," *Journal of the Geological Society*, vol. 144, no. 3, pp. 407–420, 1987.

[61] P. Guennoc, G. Pautot, and A. Coutelle, "Surficial structures of the northern Red sea axial valley from 23 N to 28 N: time and space evolution of Neo-Oceanic structures," *Tectonophysics*, vol. 153, nos. 1–4, pp. 1–23, 1988.

[62] M. Ligi, E. Bonatti, W. Bosworth, et al., "Birth of an ocean in the Red sea: Oceanic-type Basaltic melt intrusions precede Continental rupture," *Gondwana Research*, vol. 54, pp. 150–160, 2018.

[63] F. Martinez and J. R. Cochran, "Structure and Tectonics of the northern Red sea: catching a Continental margin between Rifting and drifting," *Tectonophysics*, vol. 150, nos. 1–2, pp. 1–31, 1988.

[64] S. A. Saada, K. Mickus, A. M. Eldosouky, and A. Ibrahim, "Insights on the Tectonic styles of the Red sea rift using gravity and magnetic data," *Marine and Petroleum Geology*, vol. 133, p. 105253, 2021.

[65] A. Delaunay, G. Baby, J. Fedorik, A. M. Afifi, P. Tapponnier, and J. Dyment, "Structure and morphology of the Red sea, from the mid-ocean ridge to the ocean-continent boundary," *Tectonophysics*, vol. 849, p. 229728, 2023.

[66] F. M. van der Zwan, C. W. Devey, N. Augustin, R. R. Almeev, R. A. Bantan, and A. Basaham, "Hydrothermal activity at the Ultraslow-to slow-spreading Red sea rift traced by chlorine in Basalt," *Chemical Geology*, vol. 405, pp. 63–81, 2015.

[67] J. R. Cochran, "Northern Red sea: Nucleation of an Oceanic spreading center within a Continental rift," *Geochemistry, Geophysics, Geosystems*, vol. 6, no. 3, 2005.

[68] M. Nemčok, "The role of pre-rift heat flow in thermal regimes of rifts and passive margins," in *Rifts and Passive Margins: Structural Architecture, Thermal Regimes, and Petroleum Systems*, pp. 245–255, Cambridge University Press, Cambridge, 2016.

[69] M. S. Steckler, F. Berthelot, N. Lyberis, and X. Le Pichon, "Subsidence in the Gulf of Suez: implications for Rifting and plate Kinematics," *Tectonophysics*, vol. 153, nos. 1–4, pp. 249–270, 1988.

[70] W. Bosworth and K. Burke, "Evolution of the Red sea—Gulf of Aden rift system," in *Petroleum systems of divergent continental margin basins. 2005 Gulf Coast Section SEPM Foundation 25th Bob F. Perkins Annual Research Conference*, P.J. Post, N.C. Rosen, D.L. Olson, S.L. Palmes, K.T. Lyons, and G.B. Newton, Eds., pp. 342–372, Houston, 2005.

[71] M. R. Hempton, "Constraints on Arabian plate motion and Extensional history of the Red sea," *Tectonics*, vol. 6, no. 6, pp. 687–705, 1987.

[72] X. Le Pichon and J. M. Gaulier, "The rotation of Arabia and the Levant fault system," *Tectonophysics*, vol. 153, nos. 1–4, pp. 271–294, 1988.

[73] M. Ligi, E. Bonatti, G. Bortoluzzi, et al., "Birth of an ocean in the Red sea: initial pangs," *Geochemistry, Geophysics, Geosystems*, vol. 13, no. 8, 2012.

[74] D. P. McKenzie, D. Davies, and P. Molnar, "Plate Tectonics of the Red sea and East Africa," *Nature*, vol. 226, no. 5242, pp. 243–248, 1970.

[75] G. S. Lister, M. A. Etheridge, and P. A. Symonds, "Detachment Faulting and the evolution of passive Continental margins," *Geology*, vol. 14, no. 3, 1986.

[76] D. L. James and J. G. Gerard, "Sea-floor spreading and structural evolution of Southern Red sea," *AAPG Bulletin*, vol. 56, no. 2, pp. 247–259, 1972.

[77] W. Voggenreiter, H. Hötzl, and J. Mechie, "Low-angle detachment origin for the Red sea rift system," *Tectonophysics*, vol. 150, nos. 1–2, pp. 51–75, 1988.

[78] B. Wernicke, "Uniform-sense normal simple shear of the Continental Lithosphere," *Canadian Journal of Earth Sciences*, vol. 22, no. 1, pp. 108–125, 1985.

[79] R. G. Bohannon and S. L. Eittreim, "Tectonic development of passive Continental margins of the Southern and central Red sea with a comparison to Wilkes land, Antarctica," *Tectonophysics*, vol. 198, nos. 2–4, pp. 129–154, 1991.

[80] E. Bonatti, "Punctiform initiation of Seafloor spreading in the Red sea during transition from a Continental to an Oceanic rift," *Nature*, vol. 316, no. 6023, pp. 33–37, 1985.

[81] T. V. Gerya, "Three-dimensional Thermomechanical modeling of Oceanic spreading initiation and evolution," *Physics of the Earth and Planetary Interiors*, vol. 214, pp. 35–52, 2013.

[82] T. Tentler and V. Acocella, "How does the initial configuration of Oceanic ridge segments affect their interaction? Insights from analogue models," *Journal of Geophysical Research*, vol. 115, no. B1, 2010.

[83] W. R. Buck, "Modes of Continental Lithospheric extension," *Journal of Geophysical Research*, vol. 96, no. B12, pp. 20161–20178, 1991.

[84] C. Ebinger, A. Ayele, D. Keir, et al, "Length and Timescales of rift Faulting and Magma intrusion: the afar Rifting cycle from 2005 to present," *Annual Review of Earth and Planetary Sciences*, vol. 38, no. 1, pp. 439–466, 2010.

[85] D. Keir, C. Pagli, I. D. Bastow, and A. Ayele, "The Magma-Assisted removal of Arabia in afar: evidence from Dike injection in the Ethiopian rift captured using Insar and Seismicity," *Tectonics*, vol. 30, no. 2, 2011.

[86] I. D. Bastow and D. Keir, "The protracted development of the continent–ocean transition in afar," *Nature Geoscience*, vol. 4, no. 4, pp. 248–250, 2011.

[87] K. A. Daniels, I. D. Bastow, D. Keir, R. S. J. Sparks, and T. Menand, "Thermal models of Dyke intrusion during development of continent–ocean transition," *Earth and Planetary Science Letters*, vol. 385, pp. 145–153, 2014.

[88] M. Ligi, E. Bonatti, and N. Rasul, "Seafloor spreading initiation: geophysical and Geochemical constraints from the Thetis and Nereus deeps, central Red sea," in *The Red Sea*, pp. 79–98, Springer, Berlin, Heidelberg, 2015.

[89] H. Thybo and C. A. Nielsen, "Magma-compensated Crustal thinning in Continental rift zones," *Nature*, vol. 457, no. 7231, pp. 873–876, 2009.

[90] S. C. Boone, M. L. Balestrieri, and B. Kohn, "Thermo-Tectonic imaging of the Gulf of Aden-red sea rift systems and Afro-Arabian Hinterland," *Earth-Science Reviews*, vol. 222, p. 103824, 2021.

[91] Y. Park, A. A. Nyblade, A. J. Rodgers, and A. Al-Amri, "S wave velocity structure of the Arabian shield upper Mantle from Rayleigh wave tomography," *Geochemistry, Geophysics, Geosystems*, vol. 9, no. 7, 2008.

[92] A. G. Petrunin, M. K. Kaban, S. El Khrepy, and N. Al-Arifi, "Mantle convection patterns reveal the mechanism of the Red sea Rifting," *Tectonics*, vol. 39, no. 2, 2020.

[93] K. S. Sreenidhi, P. G. Betts, M. Radhakrishna, and R. Armit, "Influence of lateral plume channel on the evolution of rift arms of the afar triple junction: constraints from 3-D gravity interpretation," *Journal of Geophysical Research*, vol. 128, no. 8, 2023.

[94] P. Japsen, J. A. Chalmers, P. F. Green, and J. M. Bonow, "Elevated, passive Continental margins: not rift shoulders, but expressions of episodic, post-rift burial and Exhumation," *Global and Planetary Change*, vols. 90–91, pp. 73–86, 2012.

[95] S.-J. Chang, M. Merino, S. Van der Lee, S. Stein, and C. A. Stein, "Mantle flow beneath Arabia offset from the opening Red sea," *Geophysical Research Letters*, vol. 38, no. 4, 2011.

[96] Z. Yao, W. D. Mooney, H. M. Zahran, and S. E. H. Youssef, "Upper Mantle velocity structure beneath the Arabian shield from Rayleigh surface wave tomography and its implications," *Journal of Geophysical Research*, vol. 122, no. 8, pp. 6552–6568, 2017.

[97] R. Huismans and C. Beaumont, "Depth-dependent extension, two-stage breakup and Cratonic Underplating at Rifted margins," *Nature*, vol. 473, no. 7345, pp. 74–78, 2011.

[98] N. J. Kusznir and G. D. Karner, "Continental Lithospheric thinning and breakup in response to Upwelling divergent Mantle flow: application to the Woodlark, Newfoundland and Iberia margins," *Geological Society, London, Special Publications*, vol. 282, no. 1, pp. 389–419, 2007.

[99] W. U. Mohriak and S. Leroy, "Architecture of Rifted Continental margins and break-up evolution: insights from the South Atlantic, North Atlantic and Red sea–Gulf of Aden conjugate margins," *Geological Society, London, Special Publications*, vol. 369, no. 1, pp. 497–535, 2013.

[100] M. G. Abdelsalam, M. M. Abdeen, H. M. Dowaidar, and R. J. Stern, "Structural evolution of the Neoproterozoic Western Allaqi–Heiani Suture, southeastern Egypt," *Precambrian Research*, vol. 124, pp. 87–104, 2003.

[101] N. E. Molnar, A. R. Cruden, and P. G. Betts, "Interactions between Propagating Rotational rift and linear Rheological Heterogeneities: insights from Three-Dimensional laboratory experiments," *Tectonics*, vol. 36, no. 3, pp. 420–443, 2017.

[102] M. Sultan, R. Becker, R. E. Arvidson, et al., "Nature of the Red sea crust: a controversy Revisited," *Geology*, vol. 20, no. 7, 1992.